First characterization of Gamkonora gas emission, North Maluku, East Indonesia

Ugan Saing, Philipson Bani, Nia Haerani, Alessandro Aiuppa, Sofyan Primulyana, Hilma Alfianti, Devy Syahbana

First characterization of Gamkonora gas emission, North Maluku, East Indonesia

Ugan B. Saing[1], Philipson Bani[2], Nia Haerani[1], Alessandro Aiuppa[3], Sofyan Primulyana[1], Hilma Alfianti[1], Devy K. Syahbana[1], Kristianto[1]

[1]Center for Volcanology and Geological Hazard Mitigation, Jl. Diponegoro No 57, Bandung, Indonesia

[2]Laboratoire Magmas et Volcans, Univ. Blaise Pascale—CNRS—IRD, OPGC, 63000 Clermont-Ferrand, France

[3]Dipartimento DiSTeM, Università di Palermo, Italy

Abstract

Gamkonora is an active volcano capable of intense manifestations that regularly forced thousands of inhabitants to flee their villages. The most extreme eruption, in 1673, was a VEI 5 event that induced pitch-dark environment over the region. Paradoxically, little is known about Gamkonora volcano and here we present the first gas measurement results obtained in September 2018 using a MultiGAS and a scanning DOAS. Results highlight a relatively small but magmatic gas with a CO_2/S_T of 3.5, in the range of high-temperature gas emissions from Indonesian volcanoes and H_2O/SO_2, CO_2/SO_2, H_2S/SO_2, and H_2/SO_2 ratios of 135, 5.6, 0.6, and 0.2 respectively. The daily gas emission budget corresponds to 129 t, 13 t, 3.4 t, 1.1 t and 0.03 t for H_2O, CO_2, SO_2, H_2S, and H_2 respectively. Bulk rock analyses indicate a basaltic-andesite to andesite source beneath Gamkonora.

Keywords: Gamkonora volcano, magmatic degassing, gas emission budget.

Introduction

The Indonesian archipelago hosts 127 active volcanoes, distributed along four distinct arcs, including Sunda, Banda, Maluku and Sulawesi-Sangihe arc (Fig.1). Seventy-seven volcanoes are currently monitored by CVGHM (Center for Volcanology and Geological Hazard Mitigation) but a large majority is still poorly studied, particularly those located on the eastern part of the archipelago. This is the case of Gamkonora (Fig.1), for which very little is known about its activity - a paradox, considering its VEI 5 type (plinian) eruption on May 20, 1673 (Siebert et al., 2010). This cataclysmic eruption has caused pitch-dark ambiance on Ternate, a big and flourished city in the 15-17 centuries, situated 70 km southwest of the volcano. The islands of Manado and Sangir, as well as the region of Mindanao (southern Philippines), have witnessed significant ashfall (Kusumadinata, 1969; Data dasar, 2011; GVP, 2013). The death toll after this eruption is unknown but it is suspected to be high (Kusumadinata, 1969; Data dasar, 2011). The eruption extensively devasted the forest and agricultural surfaces on the northeast Halmahera Island with consequences over several months. It has also been proposed that a tsunami event occurred in 1673, triggered by an earthquake and landslide at Gamkonora. This latter inundated the nearby villages along the coast (e.g., Paris et al., 2014). Hitherto the connection with the VEI 5 eruptive was not explicit. In the recent history of the volcano, only VEI 1-2 eruptions are reported (Table 1), of which some have ejected incandescent material above the summit. In 1926, a forest fire occurred following an eruption, whilst in 1981 another eruption forced 3500 inhabitants to leave their villages and during the 2007 eruption, 8400 inhabitants were evacuated by authorities (Table 1).

In 2018, the local observatory recorded increasing seismicity, which was interpreted as caused by shallow degassing activity rather than by other seismicity mechanisms (such as deep volcano-tectonic events or harmonic tremor) (personal comm. with Gamkonora observatory). We, therefore, conducted field observations at the summit of Gamkonora on September 24, 2018, which, although revealing mild (un-pressurized) gas emissions, allowed for the first time to characterize the gas composition and emission budget for the volcano. Here we report on these gas results and provide details on the summit morphology.

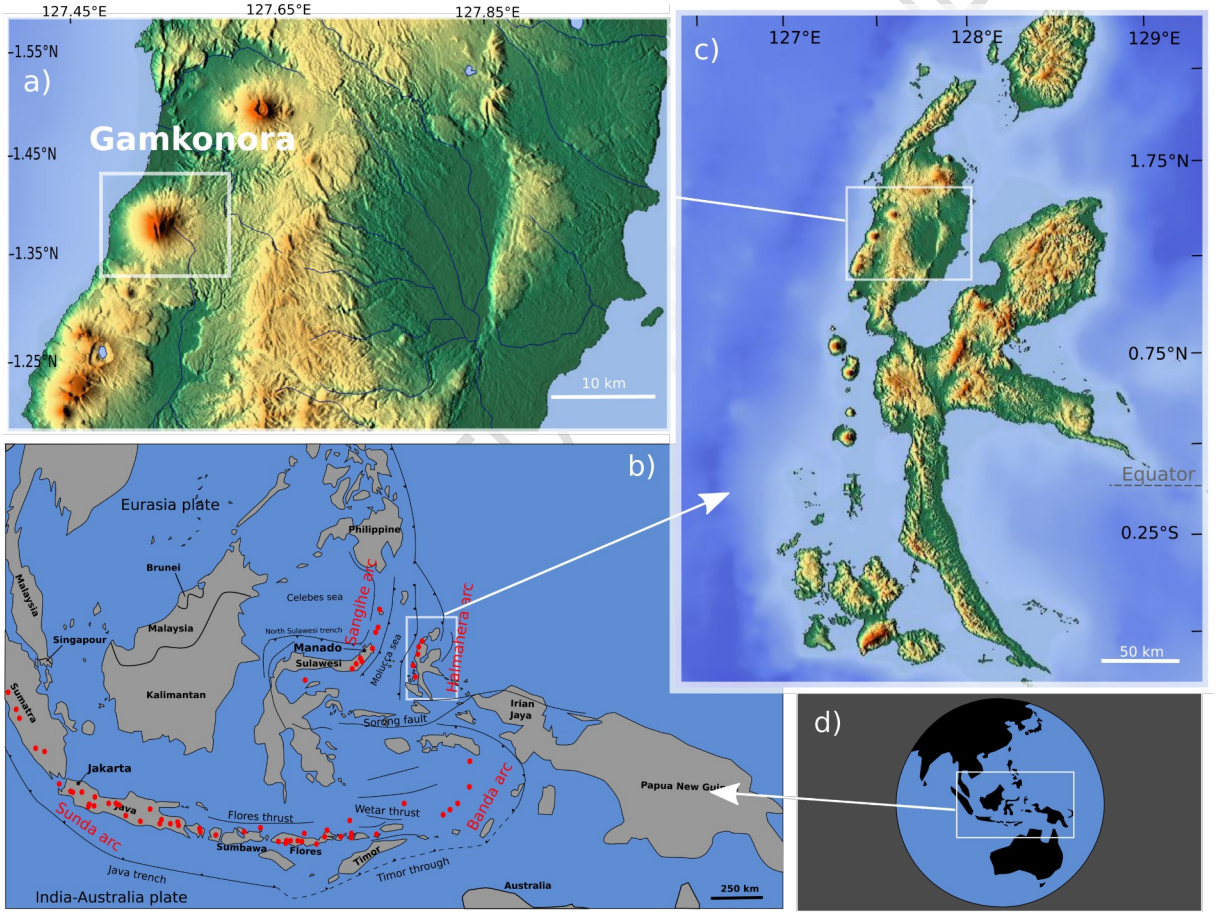

Figure 1. *Gamkonora (a) is one of the 5 active volcanoes of Halmahera arc (b) and is one of the 3 active volcanoes of Halmahea Island (c), North Maluku, east Indonesia (d).*

Table 1. Eruptive history of Gamkonora volcano

Date	Eruptive event
1564 or 1565	Strong eruption (VEI 3) at the summit crater. The blast was heard up to 200

	km from the volcano. Lava flow reached the sea and heavy ashfall has caused significant damage to the forests and cultivated land. The eruption has caused human lossbut no further information is available. Kusumadinata (1969), Data dasar (2011), GVP (2013) and Siebert et al. (2010)
1673 (May 20)	Large and massive eruption (VEI 5) have triggered a tsunami that inundated the surrounding coastal villages. The eruption was accompanied by felt earthquakes. Ash dispersal has cause pitch-dark on Ternate city. Heavy ashfall reported on Manado, Sangir Islands (North Sulawesi) and even on Mindanao (southern Philippines). Forests and agricultural surfaces were extensively devastated. The death toll related to the eruption is unknown but likely significant. Kusumadinata (1969), Data dasar (2011), GVP (2013) and Siebert et al. (2010)
1774 (Oct. 8)	Eruption at Gamkonora but no further information. Kusumadinata (1969)
1890	Eruption column above Gamkonora was visible from Ternate (VEI 2). Kusumadinata (1969) and GVP (2013)
1917 (Oct. 18)	Eruption built a thick column (VEI 2) with lightnings. Kusumadinata (1969), Data dasar (2011) and GVP (2013)
1926 (Jun. 1-2)	Explosive eruption from the central crater developing a thick plume above the crater rim. Incandescent lights were seen at night (VEI 1). Kusumadinata (1969), Data dasar (2011) and GVP (2013)
1949	Explosive eruption (VEI 2) leading to ashfall around the crater. Kusumadinata (1969), Data dasar (2011) and GVP (2013)
1950 (Oct.)	Eruption at the summit have induced forest fire around the south-southwest crater rim (VEI 2). Thick ash was observed. Kusumadinata (1969), Data dasar (2011) and GVP (2013)
1951 (Apr. 12)	Eruption sending a black plume into the atmosphere (VEI 2). Plume puff was observed from Gamsungi village. Data dasar (2011) and GVP (2013)

1952 (Jul. 16, Aug. 25, 31)	Eruption (VEI 2) developping a black column up to 1 km above the crater. Kusumadinata (1969) and GVP (2013)
1981 (Mar.-Jul.)	Eruption (VEI 1) with ash plume reaching 700 m and ashfall up to 5 km distance from the volcano. Incandescent products were seen projected above the summit. Over 3500 inhabitants fled their villages. GVP (2013) and https://www.volcanodiscovery.com/gamkonora.html
1983 (Feb. 16-17)	Ash eruption occurred but no further information. Data dasar (2011)
1987 (Apr. 13-26)	Minor ash eruptions (VEI 1) with plume reaching 700 m height. Minor ashfall on the flanks. Some coastal residents went to evacuate themselves. Data dasar (2011) and GVP (2013)
1997 (Jan. 10)	Minor ash eruption with plume reaching 200 m height above the summit (VEI 1). Data dasar (2011)
2007 (Jul. 8-11)	An eruption that commenced with a phreatic eruption then progressively became magmatic with an ash plume reaching 4000 m above the summit (VEI 2). Incandescent products were propelled 5-50 m above the crater and intermittently showered the flank. About 8,400 people were evacuated from their villages situated within 8 km radius from the volcano. GVP (2013) and Data dasar (2011)
2012 (Jun. 13)	An explosive eruption occurred in the main crater (VEI 2), plumes rose to 3000 m above the summit and ash spread out to the northeast. GVP (2013) and Suparman (2013)
2013 (Jan. 24)	An eruption in the main crater (VEI 2) produced a thick gray ash plume column that reached up to 2000-2500 m above the summit. Suparman (2013)

Methodology

To measure the gas composition at Gamkonora, we used a portable version of the Palermo-type Multi-GAS (Aiuppa et al., 2012) that measures the concentrations of CO_2, SO_2, H_2S, H_2 as well as pressure (P), temperature (T) and relative humidity (RH). This latter is then converted into H_2O concentration in the plume following Buck (1981).

The CO_2 gas is detected by non-dispersive infra-red spectroscopy (Gascard, range of 0-3,000 ppm), while SO_2, H_2S and H_2 gases are detected by specific electrochemical sensors (models 3ST/F, EZ3H, and EZT3HYT "Easy Cal" respectively, all from City Technology, with a calibration range of 0-200 ppm). The system is powered by a small internal LiPo battery (6 Ah 12 V) and collects data at a 0.5 Hz rate. On Gamkonora, the MultiGAS was positioned at the edge of the crater (Fig. 2) and was continuously recording for 2.5 h. The raw data were stored in the data logger and then processed and analyzed using the Ratiocalc software (Tamburello, 2015). Uncertainties in derived gas ratios are estimated at ≤10%, except for H_2O/SO_2 (≤30%). SO_2 flux measurements were achieved using an Ocean Optics USB2000+ spectrometer with a spectral range of 290-440 nm and a spectral resolution of 0.5 full width at half maximum. Measurements were carried out on a near-horizontal scanning mode from a fixed position (Fig. 2). The SO_2 column amounts (ppm m) were retrieved from the spectra following standard procedures outlined in Platt and Stutz (2008). Reference spectra included in the non-linear fit were obtained by convolving high-resolution SO_2 (Bogumil et al., 2003) and O_3 (Voigt et al., 2001) cross-sections with the instrument line shape. Fraunhofer reference and ring spectra were also included in the non-linear fit. The mean total column amount of the plume cross-section was then multiplied by the plume rise speed (obtained from the thermal infrared camera) to yield the SO_2 emission rate. We also deployed a miniature thermal infrared camera, the OPTRIS PI640. The camera weighs 320 g, including a

lens of 62° × 49° FOV, *f* = 8 mm, and its dynamic range equivalent to radiant temperatures from -20 to 900 °C. The detector has 640 × 480 pixels and the operating waveband is 7.5 - 13 µm with a maximum frame rate of 80 Hz (Bani et al., 2017). The camera was positioned ~60 m to the west of the main degassing vent (Fig. 2) to capture emission dynamics.

Fresh rock samples were collected in the crater then analyzed in the laboratory using X-ray fluorescence (XRF) (Johnson et al., 1999) at BPPTKG (Balai Penyelidikan dan Pengembangan Teknologi Kebencanaan Geologi) Yogyakarta-Indonesia.

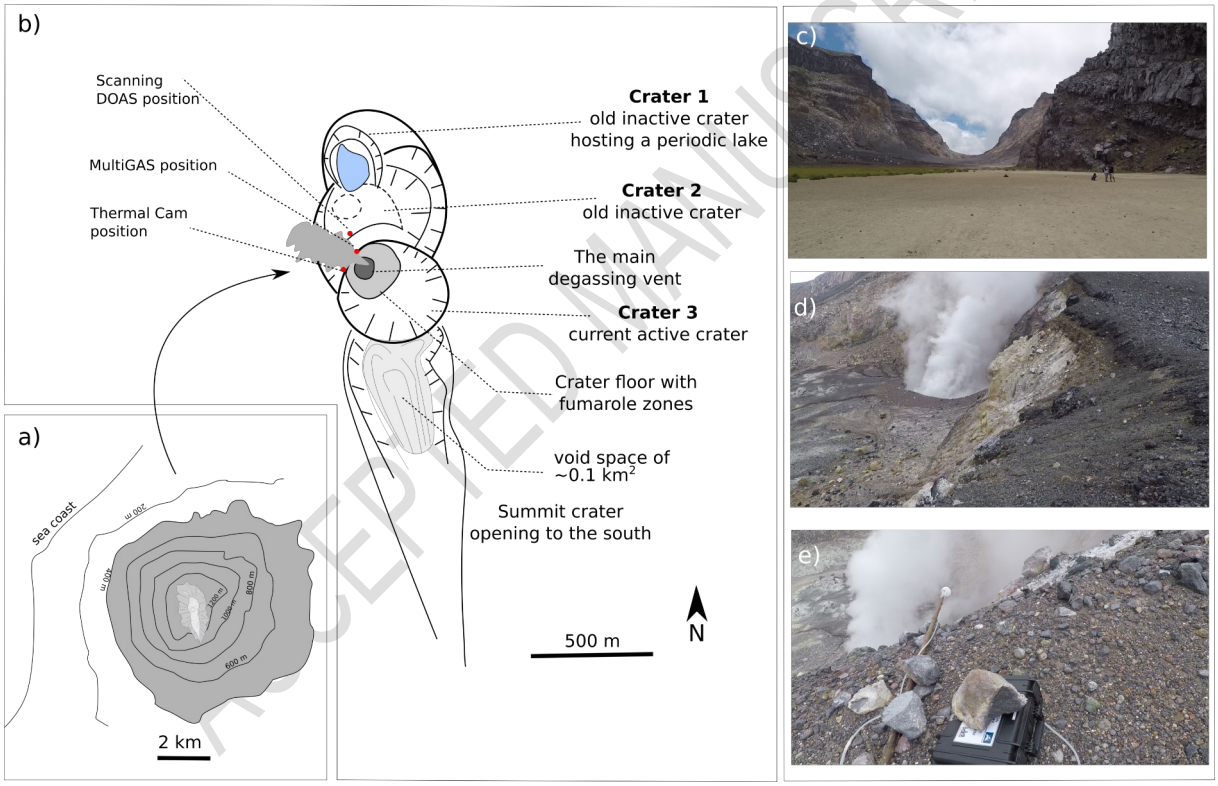

Figure 2. *Gamkonora is a large volcano that extends into the sea (a). Its summit hosts an elongated crater formed by successive emplacement of crater 1, crater 2 and crater 3 (b). Crater 1 periodically hosts a lake. Crater 3 is the currently active crater. The grey area corresponds to a possible collapsed zone. Pictures highlight the crater open to the south (c), the degassing vent (d) and the MultiGAS recording position (e).*

Results and discussion

Summit morphology: shift of active crater and possible mass failure to the south

Gamkonora is a nearly perfect cone-shaped stratovolcano that culminates at 1635 m above sea level. Its western flank extends into the sea but its aerial base diameter is about 8 km. The summit crater has an elongated shape of 1500 m x 500 m, along a north-south direction (Fig. 2). The crater is wide open to the south suggesting a crater wall failure. This latter left a void space of ~0.1 km^2. If we assume that the pre-collapse crater wall was 50 m from the rim to the floor, similar to the current situation, then one can estimate a missing volume of about 0.005 km^3 that may have collapsed from the summit of Gamkonora (Fig. 2). The age of this possible collapse event is unknown, and more work is needed to test if a link can be established between this collapse and the 1673 Gamkonora tsunami.

The summit crater of Gamkonora hosts at least 3 overlapping subcraters (Fig.2). The northernmost subcrater, named crater 1 in this work, is 250 m wide and periodically hosts a lake, in particular during the wet season. In September 2018 there was no lake allowing relatively easy access to the active crater. The biggest subcrater, situated in the central portion of the crater's terrace, is >300 m in diameter and is referred here as crater 2. Both crater 1 and 2 are currently inactive. It is unclear which of these two is the oldest. Crater 3, in contrast, has a well-preserved circular shape that cuts crater 2, suggesting a younger age (Fig.2). With 500 m diameter at the rim and 200 m on its inner crater floor, this crater 3 constitutes the current main active site on Gamkonora and is hosting the active vent from which gas exits into the atmosphere (Fig.3). Thermal images (Fig.3) highlight two distinct hot features in crater 3, including the main active degassing vent to the west and a circular structure occupying the eastern part of the crater, from which steam and dilute gases are released. Given that hot surfaces are generally sustained by deep

fluid circulations that carries heat to the surface (Chiodini et al., 2006), it is thus likely that this circular thermal distribution corresponds to an active, partially buried degassing structure whose role is now becoming secondary compared to the currently active vent. It is also possible that the activity in crater 3 has migrated to the west, in coherence with successive changes of the Gamkonora center of activity over time. Among the numerous reasons potentially causing volcanic activity shifts, subsurface emplacement of a cooled and dense magma (Primulyana et al., 2017), fault and fracture controls on magma ascent (Lanzafame et al., 2003), and/or a large mass collapse that can enhance changes in the crater, are among the most common. In any case, the elongated shape of the combined craters on top of Gamkonora suggests constant evolution of the center of activity.

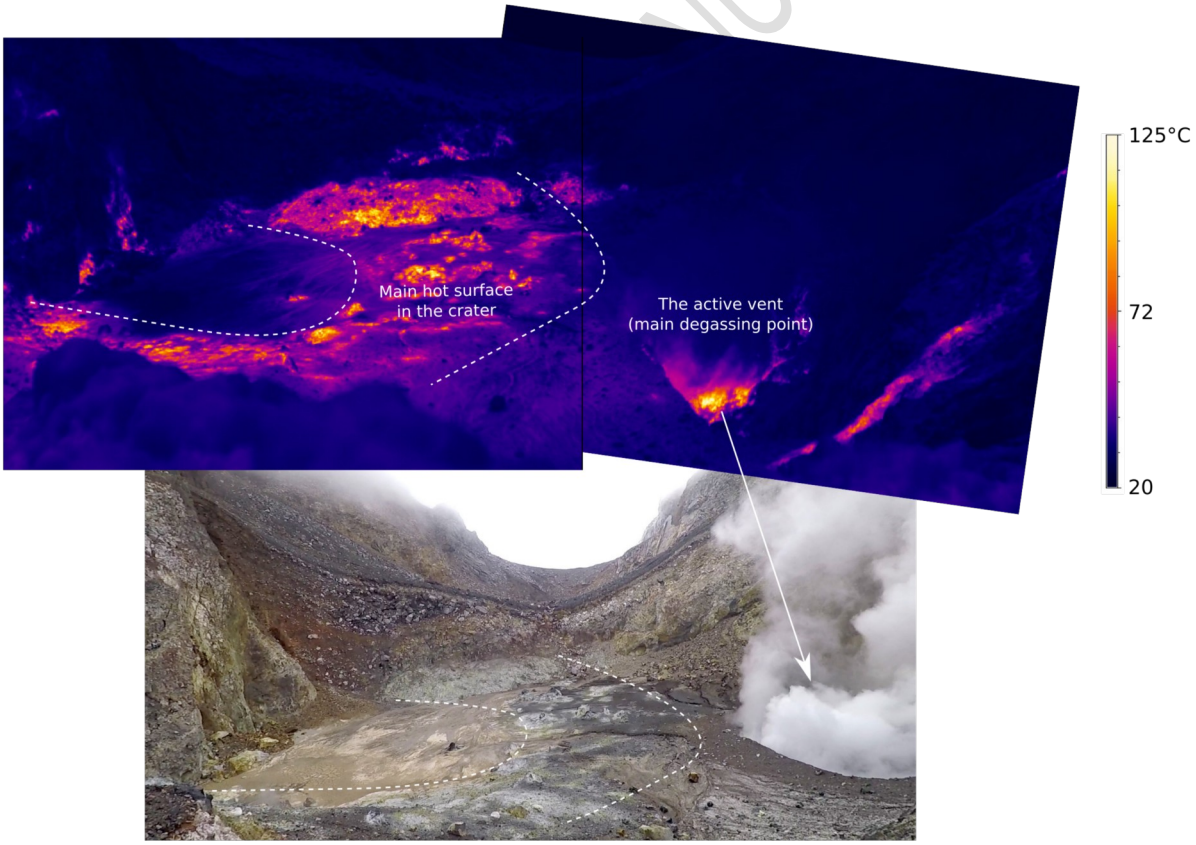

Figure 3. *Detailed view of the active crater 3. Thermal images and the corresponding picture highlight two distinct hot surfaces, including the active vent and a circular hot structure.*

Basaltic andesite to andesite melt source

The bulk rock compositions obtained from freshly ejected blocks collected next to Gamkonora crater 3 indicate basaltic-andesite to andesitic magma source (Table 2, Fig.4). Although our result is derived from a limited number of samples, and can in no way be taken as representative of the entire Gamkonora eruptive activity, it, however, suggests that at least the most recent activity has been sustained by a mildly evolved source magma, broadly within the typical volcanic arc range. Basaltic-andesitic to andesitic magma, especially if erupted after relatively long repose periods of several decades (Table 1), can enhance violent explosive eruptions. This recent Gamkonora magma composition is less differentiated compare to the magma sources at the neighboring volcanoes, Ibu and Dukono (Fig.4), located along the same arc at respectively ~15 and ~50 km to the northeast. Dukono magma is of andesite to trachy-andesite composition and is currently feeding a continuous eruptive activity (Bani et al., 2018) whilst Ibu is sustained by a dacitic source that presently undergoing lava dome build-up, associated to frequent and continuous explosive eruptions (Saing et al., 2014). Magma compositions typically evolve with time, thus it is usual to identify distinct melt sources between neighbor volcanoes and even distinct melt compositions over the eruptive history of the same volcano. A more complete petrological/volcanological rock survey, including trace-element and isotopic analyses, is urgently needed to better characterize the Gamkonora magmatic source and its evolution over the volcano's geological history.

Table 2. Rock composition of Gamkonora volcano

Oxides	Rock sample 1	Rock sample 2
SiO_2 (wt %)	55.86	58.47
Al_2O_3 (wt %)	16.96	17.05
Fe_2O_3 (wt %)	9.39	8.57

CaO (wt %)	7.09	6.73
MgO (wt %)	3.36	2.74
Na_2O (wt %)	3.78	4.02
K_2O (wt %)	1.36	1.55
TiO_2 (wt %)	0.85	0.80
MnO (wt %)	0.18	0.16
P_2O_5 (wt %)	0.21	0.24
Total	99.04	100.33

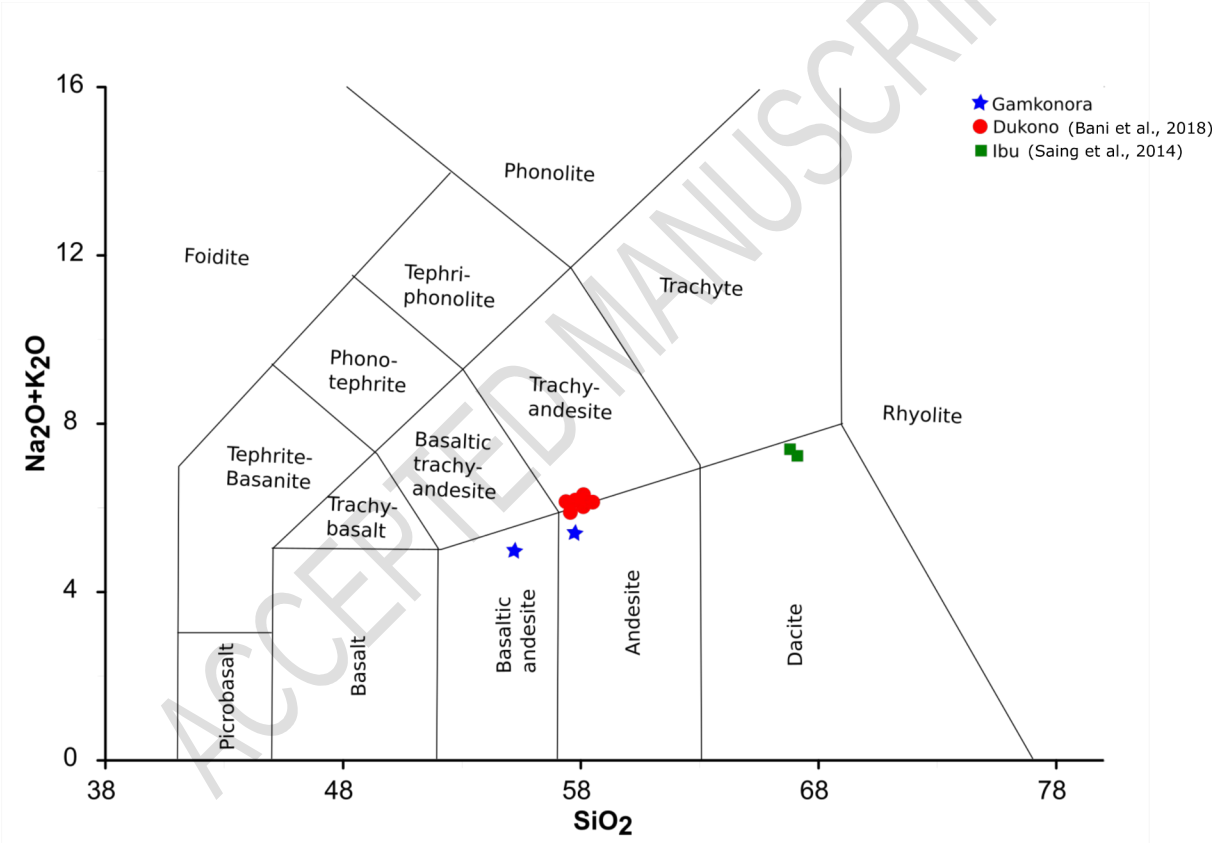

180 ***Figure 4.*** *Basaltic andesite to andesite melt composition that sustained the current Gamkonora activity. Dukono and Ibu melt sources are also plotted for comparison. These latter are more differentiated.*

A relatively small but magmatic volatile output

185 Scanning DOAS measurement results are summarized in Table 3 and indicate a mean SO_2 emission rate fluctuating between 1.6 and 6.1 t/d, with a mean value of

3.4 ± 1.4 t/d. These results thus suggest that Gamkonora is currently a weak degassing source, in comparison to other Indonesian volcanoes, including Bromo (166 t/d; Aiuppa et al. 2015), Krakatau (190 t/d; Bani et al., 2015), Dukono (820 t/d; Bani et al., 2018), Semeru (46 t/d; Smekens et al., 2015) or Sirung (48 t/d; Bani et al. 2017). Such a small gas emission suggests a quiescent activity in 2018 and is consistent with the lack of any reported eruptive event since 2013.

In-plume gas concentrations measured with the Multi-GAS (Table 4) peaked at 5500 ppmv, 418 ppmv, 5.4 ppmv, 3.5 ppmv, and 3.7 ppmv for H_2O, CO_2, SO_2, H_2S, and H_2 respectively. The good positive correlations between different gases recorded on Gamkonora (Fig.5) suggest a common. The derived ratios are circa 135, 5.6, 0.6, and 0.2 for H_2O/SO_2, CO_2/SO_2, H_2S/SO_2, and H_2/SO_2, respectively. The prevalence of SO_2 over H_2S, and the high equilibrium temperature of circa 670 ºC obtained by resolving together the SO_2/H_2S vs. H_2/H_2O redox equilibria (see methodology in Aiuppa et al., 2011; Moussallam et al., 2017; 2018), suggest that Gamkonora gas emissions are fed by a magmatic source with redox conditions between FeO-Fe_2O_3 and Nickel-Nickel Oxide buffers (NNO) (oxygen fugacity of 10^{-16} bars). The above temperature is higher than the atmospheric corrected temperature of the area around the active vent, obtained using the thermal infrared camera. Indeed, this latter peaked at 125º C (Fig.3) but should be considered minimum since a higher fluid temperature is required to compensate for the heat lost to the ambient environment along its way to the surface. When integrating the gas composition of Gamkonora on the H_2O-CO_2-S_T diagram (Fig.6), it plots next to Bromo, whose gas is considered as magmatic by Aiuppa et al (2015), but away from Papandayan with its hydrothermal system and also away from the poor-CO_2 gas of Sirung and Dukono (Bani et al. 2018). Gamkonora degassing is thus magmatic and this magmatic signature is also highlighted by the CO_2/S_T vs. gas temperature diagram (Fig.6, Aiuppa et al. 2017).

By converting our measured volatile ratios into molar percentages (in the assumption that no other major volcanogenic gas is present in addition to those we determined), we find that Gamkonora releases a water-rich gas, with 94.7% H_2O molar proportion, as typical for arc volcanic gases (Fischer, 2008). Our inferred concentrations for the other gases are 3.9%, 0.7%, 0.4% and 0.2% for CO_2, SO_2, H_2S and H_2 respectively. The mean CO_2/S_T ratio of 3.5 ($S_T = SO_2 + H_2S$) obtained for Gamkonora is above the mean arc CO_2/S_T ratio (~2) for persistently degassing open-vent arc volcanoes (Shinohara, 2013), but is well within the range of volcanic gas CO_2/S_T ratios of 3-6 in nearby Java (Aiuppa et al., 2015, 2017, 2019). Although such C-rich gas composition may be tentatively taken to imply some substantial carbon contribution from either the slab or crustal-derived fluids (Aiuppa et al., 2017, 2019) more work is yet needed to fully characterize the Maluku magmatic arc gas signature and source. This is especially true if one takes into account the CO_2-poor magmatic source observed on Dukono (Bani et al., 2018), located only ~50 km northeast of Gamkonora, which reflects the compositional heterogeneity and complex geodynamic settings of the Maluku arc.

Table 3. SO_2 flux result from DOAS scanning measurements

Scan N°	Start Time (UT)	End Time (UT)	Step angle (°)	Number of spectra	Average C.A. (g/cm²)	SO_2 Flux kg/s	SO_2 Flux t/d
1	03:37	03:41	10.0	14	0.10	0.01	1.6 ± 0.8
2	03:41	03:43	10.0	14	0.19	0.04	3.9 ± 1.1
*3**	*03:46*	*03:49*	*5.4*	*24*	*0.05*	*0.01*	*1.1 ± 1.0*
*4**	*03:49*	*03:52*	*5.4*	*24*	*0.04*	*0.01*	*0.6 ± 0.5*
5	03:53	03:57	5.4	24	0.21	0.07	6.1 ± 1.4
6	03:58	04:01	5.4	24	0.07	0.03	2.6 ± 1.7

7	04:02	04:05	5.4	24	0.08	0.04	3.7 ± 2.2
*8**	*05:03*	*05:04*	*5.4*	*24*	*0.03*	*0.01*	*0.7 ± 1.2*
9	05:06	05:09	5.4	24	0.08	0.03	2.3 ± 1.4
*10**	*05:09*	*05:12*	*5.4*	*24*	*0.03*	*0.01*	*0.8 ± 1.8*
11	*05:13*	*05:15*	*5.4*	*24*	*0.06*	*0.01*	*0.8 ± 0.7*

Mean SO_2 flux = 3.4 ± 1.4 t/d

** Scans not included in the mean SO_2 flux given the high error induced by plume direction change.*

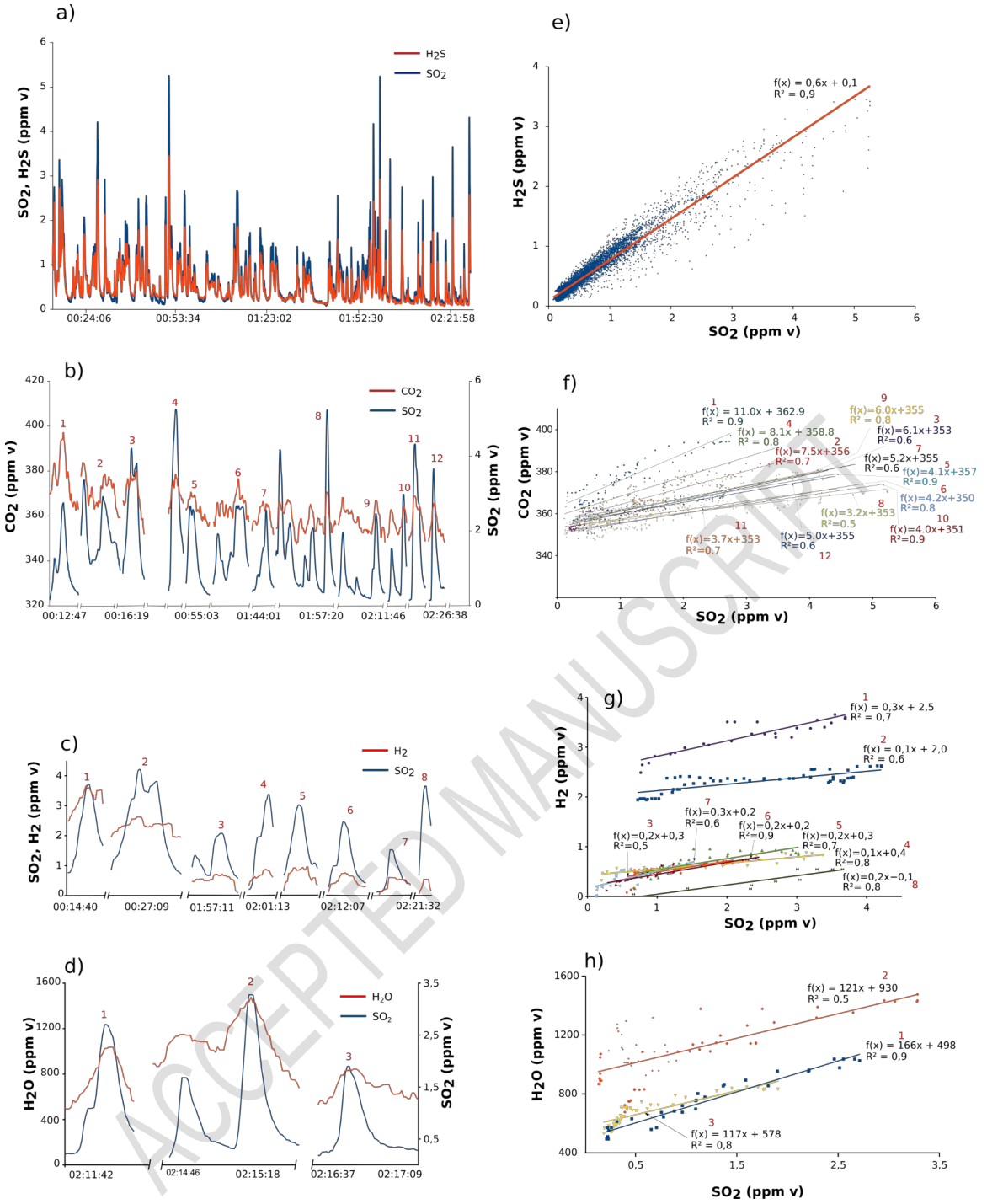

Figure 5. *Typical gas/SO2 correlation obtained on Gamkonora. Gas peaks are presented on the left panels (a, b, c , d) whilst the corresponding linear fits are presented on the right panels (e, f, g, h). SO_2 and H_2S are strongly correlated (e). All the recorded points are plotted in (a). Some of CO_2 and SO_2 peaks are well correlated (b, f), from which the mean CO_2/SO_2 ratio is obtained. Few SO_2 and H_2 peaks are correlated (c, g). There is a shift in the second part of the dataset due to a change of background condition. However, the ratios are*

comparable. A similar situation can be observed with H_2O. Only 4 acceptable SO_2-H_2O correlation peaks are retrieved (d, h).

240

Table 4. Gamkonora in-plume gas concentrations, gas ratios and fluxes

Gas concentrations		
H_2O (ppm v)	400 – 5500	
CO_2 (ppm v)	350 – 418	
SO_2 (ppm v)	0.1 – 5.4	
H_2S (ppm v)	0.1 – 3.5	
H_2 (ppm v)	0.05 – 3.7	
Gas Ratios		
H_2O/SO_2	135 ± 69	
CO_2/SO_2	5.6 ± 1.3	
H_2S/SO_2	0.6 ± 0.03	
H_2/SO_2	0.2 ± 0.1	
Gas composition and flux estimates		
	Composition (mol %)	**Flux (t/d)**
H_2O	94.7	129 ± 53
CO_2	3.9	13 ± 5
SO_2	0.7	3.4 ± 1.4
H_2S	0.4	1.1 ± 0.4
H_2	0.2	0.03 ± 0.01

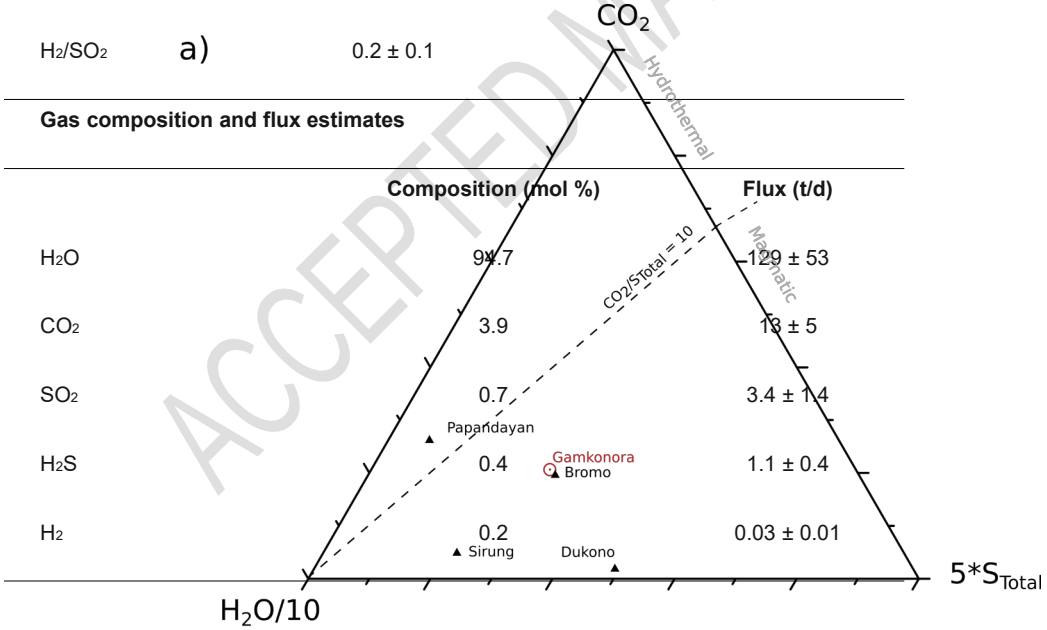

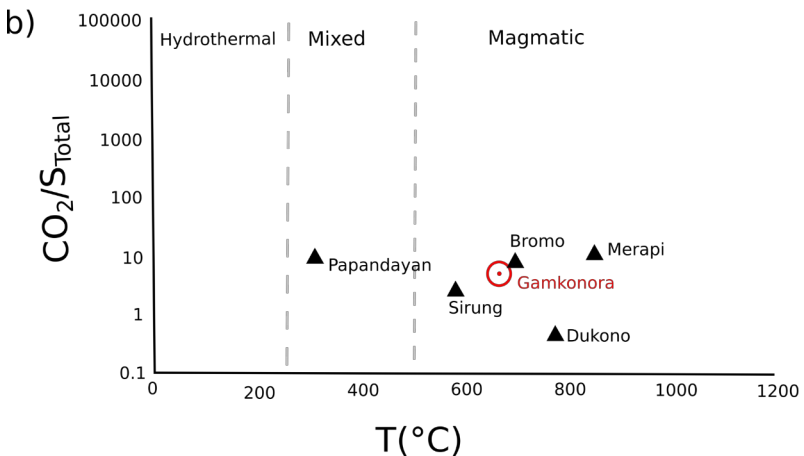

245

250

255

260

Figure 6. *CO_2-H_2O-S_T Ternary diagram (a) discriminates Gamkonora magmatic gas from the hydrothermal systems that plot along the CO_2-H_2O axis. The CO_2/ST vs. Gas temperature (T°C) (b) supports the idea of magmatic source beneath Gamkonora. Past studies have*
265 *emphasized magmatic sources on Merapi (Fisher and Chiodani, 2015), Bromo (Aippa et al., 2015), Sirung (Bani et al., 2017) and Dukono (Bani et al., 2018), whilst Papandayan is known for its hydrothermal system (Fisher and Chiodani, 2015).*

On many volcanoes with open vents, surface degassing is the result of the
270 sudden (periodic) release of over-pressured pockets of magmatic gases (Gaudin et al., 2017). In such a situation, one can expect to observe temporal fluctuations in the gas emissions and associated heat. Figure 7 illustrates a typical temporal record of discharge temperatures at the exit of Gamkonora active vent, highlighting a continuous gas emission with an apparent low frequency (0.2-0.3 Hz) and 2-6 °C
275 amplitude. Through this degassing activity, Gamkonora releases daily 129, 13, 3.4, 1.1 and 0.03 tons of H_2O, CO_2, SO_2, H_2S, and H_2 respectively (Table 3). Such volatile output accounts for a relatively small fraction of the total volcanic gas budget in

Indonesia, which includes some top-emitters such as Dukono (~820 t SO_2/d; Bani et al., 2018), Bromo (166 t SO_2/d; Aiuppa et al., 2015) or Krakatau (Bani et al., 2015).

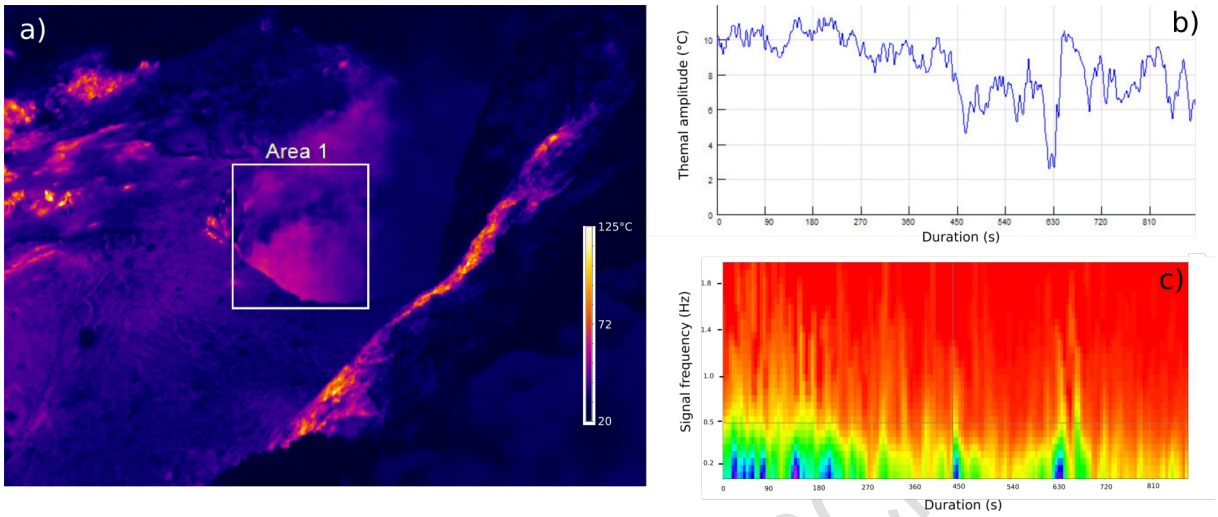

Figure 7. *Temperature fluctuation induced by hot gases that exit the active vent. The white square (a, Area 1) is the zone of interest on which the mean temperature is recorded. The temperature amplitude (b) and the spectrogram (c) denote the dynamic of degassing on Gamkonora.*

Conclusions

Gamkonora is a little known but active volcano located in North Maluku, East Indonesia. Not less than 13 eruptions have been recorded over the last 2 centuries, corresponding to about one eruption every 15 years. These eruptions forced thousands of inhabitants to leave their villages, at least temporarily. Our results, taken during quiescent activity in 2018, indicate that the current Gamkonora gas emissions are dominated by water (H_2O/SO_2 ratio of 135 ± 69), and exhibit a CO_2/S_T mean ratio (3.5) within the compositional range for high-temperature gas emissions from other Indonesian volcanoes. This degassing activity is likely supplied by basaltic-andesitic to andesitic magma at depth. In September 2018, the volcano was emitting a weak but persistent “magmatic” gas output, with daily fluxes of 129, 13,

3.4, 1.1 and 0.03 tons for H_2O, CO_2, SO_2, H_2S, and H_2 respectively. Despite the weak emissions measured, we argue that our results are significant for understanding the "characteristic" degassing behavior of the many Indonesian volcanoes that, similarly to Gamkonora, have erupted recently, but are currently undergoing quiescent degassing activity. This category may include several tens of volcanoes, whose cumulative volatile output is unknown, but may make a sizable fraction of the regional volcanic degassing budget. Quantifying the gas emissions from these (yet unmeasured) volcanoes is thus central to refining estimates of the Indonesian volcanic gas budget, and to test the representatives of the Gamkonora presented here.

Acknowledgments

The research leading to these results has received support from JEAI-COMMISSION under the collaboration between CVGHM and IRD. We acknowledge the field support from Gamkonora and Ibu observatories. We also thank the deputy editor J. Taddeucci, the associate editor T.P. Fischer and two anonymous reviewers for their helpful comments that substantially improve this manuscript.

References

Aiuppa A, Shinohara H, Tamburello G, Giudice G, Liuzzo M, Moretti R (2011) Hydrogen in the gas plume of an open-vent volcano, Mount Etna, Italy. *J. Geophys. Res. B: Solid Earth* 116 (10), B10204

Aiuppa A, Giudice G, Liuzzo M, Tamburello G, Allard P, Calabrese S, Chaplygin I, McGonigle AJS, Taran Y (2012) First volatile inventory for Gorely volcano, Kamchatka. *Geophys. Res. Lett.* 39, L06307. http://dx.doi.org/10.1029/2012GL051177

Aiuppa A, Bani P, Moussallam Y, DiNapoli R, Allard P, Gunawan H, Hendrasto M, Tamburello G (2015) First determination of magma-derived gas emissions from Bromo

volcano, eastern Java (Indonesia). *J. Volcanol. Geotherm. Res.* vol.304, p.206-213, DOI:10.1016/j.jvolgeores.2015.09.008

Aiuppa A, Fischer TP, Plank T, Robidoux P, Di Napoli R (2017). Along-arc and inter-arc variations in volcanic gas CO_2/ST ratios reveal dual source of carbon in arc volcanism. *Earth-Science Reviews*, 168, pp. 24–47

Aiuppa A, Fischer TP, Plank T, Bani P (2019) CO_2 flux emissions from the Earth's most actively degassing volcanoes, 2005–2015. *Scientific Reports*, 9 (5442)

Bani P, Normier A, Bacri C, Allard P, Gunawan H, Hendrasto M, Surono, Tsanev V (2015) First measurement of the volcanic gas output from Anak Krakatau, Indonesia. J. Volcanol. Geotherm. Res. vol.302, p.237-241, DOI:10.1016/j.jvolgeores.2015.07.008

Bani P, Alfianti H, Aiuppa A, Oppenheimer C, Sitinjak P, Tsanev V, Saing U.B. (2017). First study of heat and gas budget for Sirung volcano, Indonesia. *Bulletin of Volcanology,* 79(8):60. https://doi.org/10.1007/s00445-017-1142-8.

Bani P, Tamburello G, Rose-Koga E, Liuzzo M, Aiuppa A, Cluzel N, Amat I, Syahbana DK, Gunawan H, Bitetto M (2018) Dukono, the predominant source of volcanic degassing in Indonesia, sustained by a depleted Indian-MORB. *Bulletin of Volcanology* 80, 5, DOI:10.1007/s00445-017-1178-9

Bogumil K, Orphal J, Homann T, Voigt S, Spietz P, Fleischmann OC, Vogel A, Harmann M, Kromminga H, Bovensmann H, Frerick J, Burrows JP (2003) Measurements of molecular absorption spectra with SCIAMACHY preflight model: instrument characterization and reference data for atmospheric remote sensing in the 230-2380 nm region. *J. Photochem. Photobiol. A.* 157(2-3):167-184. https://doi.org/10.1016/S1010-6030(03)00062-5

Buck AL (1981) New equations for computing vapor pressure and enhancement factor. *Journal of Applied Meteorology* 20.12, pp. 1527-1532. doi: 10.1175/1520-0450(1981)020<1527:nefcvp>2.0.co;2

Chiodini G, Caliro S, Caramanna G, Granier D, Minipoli C, Morettim R, Perotta L, Ventura G (2006) Geochemistry of the Submarine Gaseous Emissions of Panarea (Aeolian Islands,

Southern Italy): Magmatic vs. Hydrothermal Origin and Implications for Volcanic Surveillance. Pure and Applied Geophysics, 163, 4, 759-780

Data Dasar Gunungapi Indonesia (2011) Kementerian Energi dan Sumber daya Mineral, Badan Geologi. edisi kedua, 401-410.

Fischer TP (2008) Fluxes of volatiles (H_2O, CO_2, N_2, Cl, F) from arc volcanoes. *Geochem. J.*, 42, 21-38

Fischer TP, Chiodini G (2015) Volcanic, Magmatic and Hydrothermal Gases. In Encyclopaedia of Volcanoes, 2nd Edition, 779–797 https://doi.org/10.1016/B978-0-12-385938-9.00045-6

Gaudin D, Taddeucci J, Scarlato P, Harris A, Bombrun M, Del Bello E, Ricci T (2017) Characteristics of puffing activity revealed by ground-based, thermal infrared imaging: the example of Stromboli Volcano (Italy). Bulletin of Volcanology 79:24, doi:10.1007/s00445-017-1108-x

Global Volcanism Program (1981) Report on Gamkonora (Indonesia). In: McClelland, L (ed.), Scientific Event Alert Network Bulletin, 6:7. Smithsonian Institution https://doi.org/10.5479/si.GVP.SEAN198107-268040

Global Volcanism Program, 2013. Gamkonora (268040), in Volcanoes of the World, v. 4.8.2. Venzke, E. (ed.). Smithsonian Institution https://doi.org/10.5479/si.GVP.VOTW4-2013

Johnson DM, Hooper PR, Conrey RM (1999). XRF analysusofrocksand minerals for major and trace elements on a single low dilution Litetraborate fused bead. JCPDS-International Centre for Diffraction Data

Kusumadinata K (1969) Kumpulan data mengenai Gunung Gamkonora di Pulau Halmahera (Maluku Utara), Direktorat Vulkanologi, 58 pp

Lanzafame G, Neri M, Acocella V, Billi A, Funiciello R, Giordano G (2003) Structural features of the July-August 2001 Mount Etna eruption: evidence for a complex magma supply system. J. Geological Society, 160, 531-544

Moussallam Y, Peters N, Masias P, Aaza F, Barnie T, Schipper CI, Curtis A, Tamburello G, Aiuppa A, Bani P, Giudice G, Pieri D, Davies AG, Oppenheimer C (2017) Magmatic gas

percolation through the old lava dome of El Misti volcano. Bull. Volcanol. 79:46, doi: 10.1007/s00445-017-1129-5

Moussallam Y, Bani P, Schipper CI, Cardona C, Franco L, Barnie T, Amigo A, Curtis A, Peters N, Aiuppa A, Giudice G, Oppenheimer C (2018) Unrest at the Nevados de Chillán volcanic complex: a failed or yet to unfold magmatic eruption? Volcanica 1(1): 19-32. doi: 10.30909/vol.01.01.1932

Paris R, Switzer AD, Belousova M, Belousov A, Ontowirjo B, Whelley PL, Ulvrova M (2014) Volcanic tsunami: a review of source mechanisms, past events and hazards in Southeast Asia (Indonesia, Philippines, Papua New Guinea). Nat Hazards 70:447–470, DOI 10.1007/s11069-013-0822-8

Platt U, Stutz J (2008) Differential optical absorption spectroscopy, Principles and Applications. Springer, 597 pp

Primulyana S, Bani P, Harris A (2017) The effusive-explosive transitions at Rokatenda 2012-2013: unloading by extrusion of degassed magma with lateral gas flow. Bull. Volcanol. 79: 22, doi:10.1007/s00445-017-1104-1

Saing UB, Bani P, Kristianto (2014) Ibu volcano, a center of spectacular dacite dome growth and long-term continuous eruptive discharges. J. Volcanol. Geotherm. Res. 282:36-42. https://doi.org/10.1016/j.jvolgeores.2014.06.011

Shinohara H (2013) Volatile flux from subduction zone volcanoes: insights from a detailed evaluation of the fluxes from volcanoes in Japan. J. Volcanol. Geotherm. Res. 268, 46-63

Siebert L, Simkin T, Kimberly P (2010) Volcanoes of the world, 3rd edition, Smithsonian Institution

Smekens J-F, Clarke AB, BurtonMR, Harijoko A, Wibowo HE (2015) SO2 emissions at Semeru volcano, Indonesia: Characterization and quantification of persitent and periodic explosive activity. J. Volcanol. Geotherm. Res. 300, 121-128, https://doi.org/10.1016/j.jvolgeores.2015.01.006

Suparman Y (2013) Laporan Tanggap Darurat Gunungapi Gamkonora, Maluku Utara. Pusat Vulkanologi dan Mitigasi Bencana Geologi, pp 1-7

Tamburello G (2015) Ratiocalc: Software for processing data from multicomponent volcanic gas analyzers. Computers & Geosciences 82, pp. 63–67. doi:10.1016/j.cageo.2015.05.004

Voigt S, Orphal J, Bogumil K, Burrows JP (2001) The temperature dependence (203–293 K) of the absorption cross-sections of O_3 in the 230–850 nm region measured by Fourier-transform spectroscopy. J. Photochem. Photobiol. A. 143(1):1-9. https://doi.org/10.1016/S1010-6030(01)00480-4